A microscopic model of current-induced switching of magnetization

2010 J. Phys.: Condens. Matter 22 026003

(http://iopscience.iop.org/0953-8984/22/2/026003)

J. Phys.: Condens. Matter **22** (2010) 026003 (9pp) doi:10.1088/0953-8984/22/2/026003

A microscopic model of current-induced switching of magnetization

N Sandschneider and W Nolting

Festkörpertheorie, Institut für Physik, Humboldt-Universität zu Berlin, Newtonstraße 15, 12489 Berlin, Germany

E-mail: niko.sandschneider@physik.hu-berlin.de

Received 7 October 2009
Published 9 December 2009
Online at stacks.iop.org/JPhysCM/22/026003

Abstract

The behaviour of the magnetization in a ferromagnetic metal/nonmagnetic insulator/ferromagnetic metal/paramagnetic metal tunnel junction is studied, using the nonequilibrium Keldysh formalism. The two ferromagnets are described using the single-band Hubbard model. The left one is treated in the mean field approximation and the right ferromagnet within a (nonequilibrium) spectral density approach which takes interactions beyond the mean field into account. When a voltage is applied to the junction we observe a change of the relative orientation of the two magnetizations, which can be switched from parallel to antiparallel alignment and vice versa. This switching appears in a self-consistent way, so there is no need to use half-classical methods like the Landau–Lifshitz–Gilbert equation one. The dependence of the critical voltage at which the magnetization changes its sign on the model parameters can be studied in a systematic way.

(Some figures in this article are in colour only in the electronic version)

1. Introduction

Current-induced switching of magnetization was proposed by Slonczewski and Berger independently of each other in 1996 [1, 2]. Shortly afterwards it was confirmed by several experimental groups [3–5]. The idea behind this effect is the following: electrons in the conduction band of a ferromagnet will align their spin direction with the magnetization to minimize their energy. By applying a voltage they can be transported through a nonmagnetic layer (either metallic or insulating) to a second ferromagnet. Thus there is a transfer of spin angular momentum between the ferromagnets. This can act as a torque on the second magnetization. If the current densities are high enough (typically $>10^6$–10^7 A cm^{-2}) this torque can be sufficient to destabilize the magnetization and switch its orientation relative to the first ferromagnet. Slonczewski showed that this effect can be modelled in the framework of the Landau–Lifshitz–Gilbert equation which was also used by several other authors [6–10]. However, this equation has several disadvantages. It is a semiclassical, macroscopic equation which does not take the quantum nature of spin into account. The magnetization is treated as a classical vector which can take arbitrary orientations in space. Strictly speaking, this is not correct, since it consists of averages over spins which are quantized. Another problem is that several important parameters such as the Gilbert damping are still not completely understood on a microscopic level [11, 12]. Furthermore it is hardly possible to treat the electron–electron interaction, which may play an important role for the switching, above the mean field level. To address these shortcomings we want to formulate a microscopic theory which is able to model current-induced switching of magnetization without relying on the Landau–Lifshitz–Gilbert equation.

The paper is organized in the following way. In the next section we will present the model Hamiltonian. Since it will be a non-trivial many-body problem it cannot be solved exactly. Therefore we developed an approximate solution which will be derived in section 3. The numerical results from the theory will be discussed in section 4. The paper finishes with a short summary in section 5.

2. The model

The Hamiltonian of the system is identical to the one used in [13]:

$$H = H_{\mathrm{L}} + H_{\mathrm{LI}} + H_{\mathrm{I}} + H_{\mathrm{RI}} + H_{\mathrm{R}} + H_{\mathrm{RP}} + H_{\mathrm{P}}. \quad (1)$$

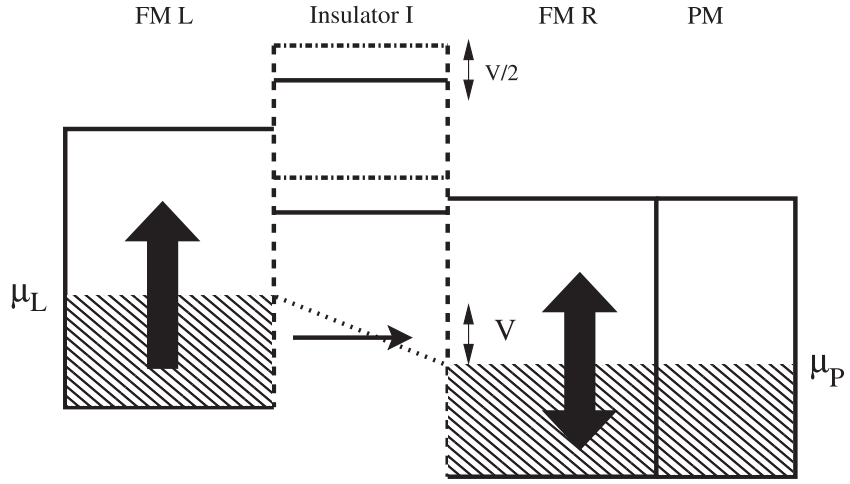

Figure 1. Schematic representation of a tunnel junction with applied voltage V. Two ferromagnets L and R are divided by an insulator I. To the right of the second ferromagnet there is a paramagnet which acts as an electron reservoir. The black arrows symbolize the magnetization direction, which is always up in the left ferromagnet and can be varied in the right one.

$H_{\mathrm{L\,(R)}}$ describes the left (right) ferromagnet, H_{I} the insulator and H_{P} the paramagnet. The two ferromagnets are given by the Hubbard Hamiltonian

$$H_M = \sum_{\mathbf{k}_M\sigma}(\epsilon_{\mathbf{k}_M} - V_M)c^{\dagger}_{\mathbf{k}_M\sigma}c_{\mathbf{k}_M\sigma} + \frac{U_M}{2}\sum_{i_M\sigma}\hat{n}_{i_M\sigma}\hat{n}_{i_M-\sigma}, \quad (2)$$

where M stands for either L or R. $c^{(\dagger)}_{\mathbf{k}_M\sigma}$ is the annihilation (creation) operator of an electron with wavevector $\mathbf{k}_M$ and spin σ in the region M. The Hubbard-U_M determines the interaction strength, $\hat{n}_{i_M\sigma} = c^{\dagger}_{i_M\sigma}c_{i_M\sigma}$ is the occupation number operator and V_M is a voltage-dependent shift of the centre of gravity.

The insulator and paramagnet are assumed to be non-interacting. Thus they are described by the following Hamiltonian:

$$H_X = \sum_{\mathbf{k}_X\sigma}(\epsilon_{\mathbf{k}_X} - V_X)d^{\dagger}_{\mathbf{k}_X\sigma}d_{\mathbf{k}_X\sigma} \qquad (X = \mathrm{I, P}). \quad (3)$$

The construction operators in the non-interacting regions are denoted by the letter d. V_X is the shift of the centre of gravity which is a result of the applied voltage V. We choose $V_{\mathrm{L}} = 0$, $V_{\mathrm{I}} = V/2$, $V_{\mathrm{R}} = V$ and $V_{\mathrm{P}} = V$. This choice will lead to the behaviour shown in figure 1. The sign convention is chosen in such a way that positive (negative) V will shift the right regions to lower (higher) energies compared to the left ferromagnet whose centre of gravity defines the zero point of energy.

In order to get a finite current through the junction the four regions have to be coupled. This is modelled by a hybridization between neighbouring regions ($M = \mathrm{L, R}$; $X = \mathrm{I, P}$):

$$H_{MX} = \sum_{\mathbf{k}_M\mathbf{k}_X\sigma}(\epsilon_{\mathbf{k}_M\mathbf{k}_X}c^{\dagger}_{\mathbf{k}_M\sigma}d_{\mathbf{k}_X\sigma} + \mathrm{h.c.}). \quad (4)$$

The strength of the hybridization is determined by the coupling constants $\epsilon_{\mathbf{k}_M\mathbf{k}_X}$ which we assume to be wavevector independent and real, i.e. $\epsilon_{\mathbf{k}_M\mathbf{k}_X} \equiv \epsilon_{MX} \equiv \epsilon_{XM}$. They will be treated as parameters since it is not possible to determine them self-consistently within the proposed theory. Since H_{MX} couples regions with different chemical potentials the system will be out of equilibrium and the Keldysh formalism [14] has to be used for the subsequent calculations.

The central quantity for the discussion of current-induced switching of magnetization is the nonequilibrium magnetization m_{R} of the right ferromagnet. It can be expressed through a lesser Green function defined as $G^{<}_{\mathbf{k}_{\mathrm{R}}\sigma}(t,t') = \mathrm{i}\langle c^{\dagger}_{\mathbf{k}_{\mathrm{R}}\sigma}(t')c_{\mathbf{k}_{\mathrm{R}}\sigma}(t)\rangle$ in the following way:

$$\begin{aligned} m_{\mathrm{R}} &= n_{\mathrm{R},\uparrow} - n_{\mathrm{R},\downarrow} \\ &= \frac{1}{2\pi\mathrm{i}N}\int_{-\infty}^{\infty}\mathrm{d}E\sum_{\mathbf{k}_{\mathrm{R}}}\left[G^{<}_{\mathbf{k}_{\mathrm{R}}\uparrow}(E) - G^{<}_{\mathbf{k}_{\mathrm{R}}\downarrow}(E)\right], \end{aligned} \quad (5)$$

where $n_{\mathrm{R},\sigma} = \langle\hat{n}_{\mathrm{R},\sigma}\rangle$ is the occupation number of particles with spin σ in the right ferromagnet. The first step for calculating the lesser Green function is to determine the retarded one, $G^{\mathrm{r}}_{\mathbf{k}_{\mathrm{R}}\sigma}(E) = \langle\langle c_{\mathbf{k}_{\mathrm{R}}\sigma}; c^{\dagger}_{\mathbf{k}_{\mathrm{R}}\sigma}\rangle\rangle^{\mathrm{r}}_{E}$. This task can be solved in a straightforward way by the use of the equation of motion method. One finds for the Green function

$$G^{\mathrm{r}}_{\mathbf{k}_{\mathrm{R}}\sigma}(E) = \frac{1}{E - \epsilon_{\mathbf{k}_{\mathrm{R}}} - \Sigma^{\mathrm{r}}_{\mathbf{k}_{\mathrm{R}}\sigma}(E) - \Delta^{\mathrm{r}}_{\mathbf{k}_{\mathrm{R}}\sigma}(E)}. \quad (6)$$

The two different self-energies which appear in the denominator are related to the interactions due to the Hubbard term ($\Sigma^{\mathrm{r}}_{\mathbf{k}_{\mathrm{R}}\sigma}(E)$) and the transport due to the hybridization ($\Delta^{\mathrm{r}}_{\mathbf{k}_{\mathrm{R}}\sigma}(E)$). The interaction self-energy is defined in the usual way:

$$\Sigma^{\mathrm{r}}_{\mathbf{k}_{\mathrm{R}}\sigma}(E)G^{\mathrm{r}}_{\mathbf{k}_{\mathrm{R}}\sigma}(E) = \langle\langle[c_{\mathbf{k}_{\mathrm{R}}\sigma}, H^{\mathrm{int}}_{\mathrm{R}}]_{-}; c^{\dagger}_{\mathbf{k}_{\mathrm{R}}\sigma}\rangle\rangle^{\mathrm{r}}_{E}, \quad (7)$$

where $H^{\mathrm{int}}_{\mathrm{R}}$ is the Hubbard part of the Hamiltonian (2). The transport self-energy follows immediately from the equation of motion approach. Thus we will just state the results here. Its retarded and lesser components are given by

$$\Delta^{\mathrm{r(<)}}_{\mathbf{k}_{\mathrm{R}}\sigma}(E) = \sum_{\mathbf{k}_{\mathrm{I}}}\epsilon^2_{M\mathrm{I}}G^{\mathrm{(L),r(<)}}_{\mathbf{k}_{\mathrm{I}}\sigma}(E) + \sum_{\mathbf{k}_{\mathrm{P}}}\epsilon^2_{\mathrm{RP}}g^{\mathrm{r(<)}}_{\mathbf{k}_{\mathrm{P}}\sigma}(E) \quad (8)$$

$G^{(\mathrm{L}),\mathrm{r}(<)}_{\mathbf{k}_\mathrm{I}\sigma}(E)$ is the Green function of the insulator when it is only coupled to the left ferromagnet:

$$G^{(\mathrm{L}),\mathrm{r}}_{\mathbf{k}_\mathrm{I}\sigma}(E) = \frac{1}{E - \epsilon_{\mathbf{k}_\mathrm{I}} - \sum_{\mathbf{k}_\mathrm{L}} \epsilon^2_{MI} g^{\mathrm{r}}_{\mathbf{k}_\mathrm{L}\sigma}(E)}. \tag{9}$$

The equilibrium Green functions of the left ferromagnet and the paramagnet, $g^{\mathrm{r}}_{\mathbf{k}_\mathrm{L}\sigma}(E)$ and $g^{\mathrm{r}}_{\mathbf{k}_\mathrm{P}\sigma}(E)$, are given by

$$g^{\mathrm{r}}_{\mathbf{k}_M\sigma}(E) = \frac{1}{E - \epsilon_{\mathbf{k}_M} - \Sigma^{\mathrm{r}}_{\mathbf{k}_M\sigma}(E)} \qquad (M = \mathrm{L}, \mathrm{P}). \tag{10}$$

Since the paramagnet is assumed to be non-interacting its self-energy is simply $\Sigma^{\mathrm{r}}_{\mathbf{k}_\mathrm{P}\sigma}(E) = -\mathrm{i}0^+$. The self-energy of the left ferromagnet which is not trivial due to the interactions will be specified later on. Now that the retarded Green function is known, the lesser Green function follows from the Keldysh equation which in this case reads [15]

$$G^{<}_{\mathbf{k}_\mathrm{R}\sigma}(E) = \left(\Sigma^{<}_{\mathbf{k}_\mathrm{R}\sigma}(E) + \Delta^{<}_{\mathbf{k}_\mathrm{R}\sigma}(E)\right) |G^{\mathrm{r}}_{\mathbf{k}_\mathrm{R}\sigma}(E)|^2. \tag{11}$$

The lesser transport self-energy was already given in (8) where the lesser components of the two Green functions on the right-hand side are

$$G^{(\mathrm{L}),<}_{\mathbf{k}_\mathrm{I}\sigma}(E) = \sum_{\mathbf{k}_\mathrm{L}} \epsilon^2_{MI} g^{<}_{\mathbf{k}_\mathrm{L}\sigma}(E) |G^{(\mathrm{L}),\mathrm{r}}_{\mathbf{k}_\mathrm{I}\sigma}(E)|^2 \tag{12}$$

and

$$g^{<}_{\mathbf{k}_M\sigma}(E) = -2\mathrm{i} f_M(E)\, \mathrm{Im}\, g^{\mathrm{r}}_{\mathbf{k}_M\sigma}(E) \qquad (M = \mathrm{L}, \mathrm{P}). \tag{13}$$

$f_M(E)$ is the Fermi function of the lead M with chemical potential μ_M. The potentials are closely connected to the applied voltage by the relation $\mu_\mathrm{L} - \mu_\mathrm{P} = V$. Apart from the interaction self-energies the above expressions form a closed set of equations for calculating the magnetization of the switching ferromagnet. The determination of the right interaction self-energy is no easy task, due to the fact that the Hubbard model is not exactly solvable and that one cannot use equilibrium relations, such as the spectral theorem, which often play an important role for the self-energy calculations. These difficulties can be overcome by a so-called nonequilibrium spectral density approach (NSDA) which we will present in detail in the next part of the paper.

3. The NSDA

The NSDA is based on a high-energy expansion of the retarded Green function. By means of its spectral representation, which still holds in nonequilibrium, it can be expressed using the spectral density $S_{\mathbf{k}_\mathrm{R}\sigma}(t,t') = \frac{1}{2\pi}\langle[c_{\mathbf{k}_\mathrm{R}\sigma}(t), c^\dagger_{\mathbf{k}_\mathrm{R}\sigma}(t')]_+\rangle$:

$$\begin{aligned} G^{\mathrm{r}}_{\mathbf{k}_\mathrm{R}\sigma}(E) &= \int_{-\infty}^{\infty} \mathrm{d}E' \frac{S_{\mathbf{k}_\mathrm{R}\sigma}(E')}{E - E'} \\ &= \frac{1}{E}\int_{-\infty}^{\infty} \mathrm{d}E' \frac{S_{\mathbf{k}_\mathrm{R}\sigma}(E')}{1 - \frac{E'}{E}} \\ &= \frac{1}{E}\sum_{n=0}^{\infty}\int_{-\infty}^{\infty} \mathrm{d}E' \left(\frac{E'}{E}\right)^n S_{\mathbf{k}_\mathrm{R}\sigma}(E') \\ &= \sum_{n=0}^{\infty} \frac{M^{(n)}_{\mathbf{k}_\mathrm{R}\sigma}}{E^{n+1}}. \end{aligned} \tag{14}$$

In the last step the definition of the spectral moments

$$M^{(n)}_{\mathbf{k}_\mathrm{R}\sigma} = \int_{-\infty}^{\infty} \mathrm{d}E E^n S_{\mathbf{k}_\mathrm{R}\sigma}(E) \qquad n = 0, 1, 2, \ldots \tag{15}$$

was used. Alternatively the moments can be calculated using the following relation:

$$\begin{aligned} M^{(n)}_{\mathbf{k}_\mathrm{R}\sigma} = \langle[[\ldots[[c_{\mathbf{k}_\mathrm{R}\sigma}, H]_-, H]_- \ldots, H]_-, \\ [H, \ldots[H, c^\dagger_{\mathbf{k}_\mathrm{R}\sigma}]_- \ldots]_-]_+\rangle. \end{aligned} \tag{16}$$

The total number of commutators within the anticommutator on the right-hand side has to be equal to n. This relation is quite useful because it allows one, at least in principle, to calculate the moments exactly to arbitrary order with a given Hamiltonian. The Green function (6) can be rewritten as

$$E G^{\mathrm{r}}_{\mathbf{k}_\mathrm{R}\sigma}(E) = 1 + (\epsilon_{\mathbf{k}_\mathrm{R}} + \Sigma^{\mathrm{r}}_{\mathbf{k}_\mathrm{R}\sigma}(E) + \Delta^{\mathrm{r}}_{\mathbf{k}_\mathrm{R}\sigma}(E)) G^{\mathrm{r}}_{\mathbf{k}_\mathrm{R}\sigma}(E). \tag{17}$$

Inserting the expansion (14) and the corresponding expansions for the self-energies

$$\Sigma^{\mathrm{r}}_{\mathbf{k}_\mathrm{R}\sigma}(E) = \sum_{m=0}^{\infty} \frac{C^{(m)}_{\mathbf{k}_\mathrm{R}\sigma}}{E^m}, \qquad \Delta^{\mathrm{r}}_{\mathbf{k}_\mathrm{R}\sigma}(E) = \sum_{m=0}^{\infty} \frac{D^{(m)}_{\mathbf{k}_\mathrm{R}\sigma}}{E^m} \tag{18}$$

into this expression yields a system of equations for the unknown coefficients $C^{(m)}_{\mathbf{k}_\mathrm{R}\sigma}$ which determine the interaction self-energy. Since the spectral moments on each side of the equation are not energy dependent, the relation can only hold if the prefactors of the $1/E$ terms are identical in every power of n. Comparing them leads to the following expressions for the first few self-energy coefficients:

$$C^{(0)}_{\mathbf{k}_\mathrm{R}\sigma} = \frac{M^{(1)}_{\mathbf{k}_\mathrm{R}\sigma}}{M^{(0)}_{\mathbf{k}_\mathrm{R}\sigma}} - \epsilon_{\mathbf{k}_\mathrm{R}} - D^{(0)}_{\mathbf{k}_\mathrm{R}\sigma} \tag{19}$$

$$C^{(1)}_{\mathbf{k}_\mathrm{R}\sigma} = \frac{M^{(2)}_{\mathbf{k}_\mathrm{R}\sigma}}{M^{(0)}_{\mathbf{k}_\mathrm{R}\sigma}} - \left(\frac{M^{(1)}_{\mathbf{k}_\mathrm{R}\sigma}}{M^{(0)}_{\mathbf{k}_\mathrm{R}\sigma}}\right)^2 - D^{(1)}_{\mathbf{k}_\mathrm{R}\sigma} \tag{20}$$

$$C^{(2)}_{\mathbf{k}_\mathrm{R}\sigma} = \frac{M^{(3)}_{\mathbf{k}_\mathrm{R}\sigma}}{M^{(0)}_{\mathbf{k}_\mathrm{R}\sigma}} - 2\frac{M^{(1)}_{\mathbf{k}_\mathrm{R}\sigma} M^{(2)}_{\mathbf{k}_\mathrm{R}\sigma}}{(M^{(0)}_{\mathbf{k}_\mathrm{R}\sigma})^2} + \left(\frac{M^{(1)}_{\mathbf{k}_\mathrm{R}\sigma}}{M^{(0)}_{\mathbf{k}_\mathrm{R}\sigma}}\right)^3 - D^{(2)}_{\mathbf{k}_\mathrm{R}\sigma}. \tag{21}$$

To solve these equations one needs the first four moments of the right ferromagnet and the first three moments of the transport self-energy. But even without their explicit knowledge one can make some important statements. The ansatz (18) will always lead to a real self-energy, i.e. quasiparticle damping cannot be taken into account by this method. The advanced and retarded self-energies will thus be equal, $\Sigma^{\mathrm{r}}_{\mathbf{k}_\mathrm{R}\sigma}(E) = \Sigma^{a}_{\mathbf{k}_\mathrm{R}\sigma}(E)$. Additionally one can show, e.g. by using the ansatz of Ng [16], that real self-energies always lead to vanishing lesser self-energies, i.e. $\Sigma^{<}_{\mathbf{k}_\mathrm{R}\sigma}(E) = 0$. Therefore the Keldysh equation can be simplified to

$$G^{<}_{\mathbf{k}_\mathrm{R}\sigma}(E) = \Delta^{<}_{\mathbf{k}_\mathrm{R}\sigma}(E) |G^{\mathrm{r}}_{\mathbf{k}_\mathrm{R}\sigma}(E)|^2. \tag{22}$$

The next step will be the calculation of the spectral moments of the right ferromagnet which are given by

$$\begin{aligned} M^{(n)}_{\mathbf{k}_\mathrm{R}\sigma} = \frac{1}{N}\sum_{i_\mathrm{R} j_\mathrm{R}} \mathrm{e}^{-\mathrm{i}\mathbf{k}_\mathrm{R}\cdot(\mathbf{R}_{i_\mathrm{R}} - \mathbf{R}_{j_\mathrm{R}})} \langle[[\ldots[c_{i_\mathrm{R}\sigma}, H]_- \ldots, H]_-, \\ [H \ldots[H, c^\dagger_{j_\mathrm{R}\sigma}]_- \ldots]_-]_+\rangle. \end{aligned} \tag{23}$$

This is a tedious but straightforward procedure. Here, we will give only the results:

$$M^{(0)}_{\mathbf{k}_\mathrm{R}\sigma} = 1 \tag{24}$$

$$M^{(1)}_{\mathbf{k}_\mathrm{R}\sigma} = \epsilon_{\mathbf{k}_\mathrm{R}} + U_\mathrm{R} n_{\mathrm{R},-\sigma} \tag{25}$$

$$M^{(2)}_{\mathbf{k}_\mathrm{R}\sigma} = \epsilon^2_{\mathbf{k}_\mathrm{R}} + 2U_\mathrm{R}\epsilon_{\mathbf{k}_\mathrm{R}} n_{\mathrm{R},-\sigma} + U^2_\mathrm{R} n_{\mathrm{R},-\sigma} + \sum_{X=\mathrm{I,P}} \epsilon^2_{\mathrm{R}X} \tag{26}$$

$$\begin{aligned} M^{(3)}_{\mathbf{k}_\mathrm{R}\sigma} &= \epsilon^3_{\mathbf{k}_\mathrm{R}} + \sum_{X=\mathrm{I,P}} \left(2\epsilon_{\mathbf{k}_\mathrm{R}}\epsilon^2_{\mathrm{R}X} + T_{0,X}\epsilon^2_{\mathrm{R}X}\right) \\ &\quad + U_\mathrm{R}\left\{3\epsilon^2_{\mathbf{k}_\mathrm{R}} n_{\mathrm{R},-\sigma} + 2\sum_{X=\mathrm{I,P}} \epsilon^2_{\mathrm{R}X} n_{\mathrm{R},-\sigma} + B_{1,-\sigma}(\mathbf{k}_\mathrm{R})\right\} \\ &\quad + U^2_\mathrm{R}\{((2+n_{\mathrm{R},-\sigma})\epsilon_{\mathbf{k}_\mathrm{R}} + T_{0,\mathrm{R}})n_{\mathrm{R},-\sigma} + B_{S,-\sigma} + B_{T,-\sigma} \\ &\quad + B_{W,-\sigma}(\mathbf{k}_\mathrm{R})\} + U^3_\mathrm{R} n_{\mathrm{R},-\sigma}. \end{aligned} \tag{27}$$

$T_{0,X}$ is the centre of gravity of the band in region X and the band corrections which appear in the third moment are defined as

$$\begin{aligned} B_{1,-\sigma}(\mathbf{k}_\mathrm{R}) &= \frac{1}{N}\sum_{X=\mathrm{I,P}}\sum_{i_\mathrm{R} j_\mathrm{R} i_X} \mathrm{e}^{-\mathrm{i}\mathbf{k}_\mathrm{R}\cdot(\mathbf{R}_{i_\mathrm{R}}-\mathbf{R}_{j_\mathrm{R}})} T_{i_\mathrm{R} j_\mathrm{R}} \\ &\quad \times (T_{i_\mathrm{R} i_X}\langle c^\dagger_{i_\mathrm{R}-\sigma} d_{i_X-\sigma}\rangle - T_{i_X i_\mathrm{R}}\langle d^\dagger_{i_X-\sigma} c_{i_\mathrm{R}-\sigma}\rangle) \end{aligned} \tag{28}$$

$$B_{S,-\sigma} = \frac{1}{N}\sum_{i_\mathrm{R} j_\mathrm{R}} T_{i_\mathrm{R} j_\mathrm{R}}\langle c^\dagger_{i_\mathrm{R}-\sigma} c_{j_\mathrm{R}-\sigma}(2n_{i_\mathrm{R}\sigma} - 1)\rangle \tag{29}$$

$$B_{T,-\sigma} = \frac{1}{N}\sum_{X=\mathrm{I,P}}\sum_{i_\mathrm{R} i_X} T_{i_X i_\mathrm{R}}\langle d^\dagger_{i_X-\sigma} c_{i_\mathrm{R}-\sigma}(2n_{i_\mathrm{R}\sigma} - 1)\rangle \tag{30}$$

$$\begin{aligned} B_{W,-\sigma}(\mathbf{k}_\mathrm{R}) &= \frac{1}{N}\sum_{i_\mathrm{R} j_\mathrm{R}} T_{i_\mathrm{R} j_\mathrm{R}} \mathrm{e}^{-\mathrm{i}\mathbf{k}_\mathrm{R}\cdot(\mathbf{R}_{i_\mathrm{R}}-\mathbf{R}_{j_\mathrm{R}})}(\langle \hat{n}_{i_\mathrm{R}-\sigma}\hat{n}_{j_\mathrm{R}-\sigma}\rangle \\ &\quad - n^2_{\mathrm{R},-\sigma} - \langle c^\dagger_{j_\mathrm{R}\sigma} c^\dagger_{j_\mathrm{R}-\sigma} c_{i_\mathrm{R}-\sigma} c_{i_\mathrm{R}\sigma}\rangle - \langle c^\dagger_{j_\mathrm{R}\sigma} c^\dagger_{i_\mathrm{R}-\sigma} c_{j_\mathrm{R}-\sigma} c_{i_\mathrm{R}\sigma}\rangle). \end{aligned} \tag{31}$$

All the correlation functions which appear in the above equations have to be calculated within the Keldysh formalism. For $B_{1,-\sigma}(\mathbf{k}_\mathrm{R})$ this is quite easy, because it can be reduced to another known quantity. Fourier transformation to the wavevector dependence leads to

$$\begin{aligned} B_{1,-\sigma}(\mathbf{k}_\mathrm{R}) &= \frac{1}{N}\sum_{X=\mathrm{I,P}}\sum_{\mathbf{q}_\mathrm{R}\mathbf{k}_X} \epsilon_{\mathbf{k}_\mathrm{R}}(\epsilon_{\mathrm{R}X}\langle c^\dagger_{\mathbf{q}_\mathrm{R}-\sigma} d_{\mathbf{k}_X-\sigma}\rangle \\ &\quad - \epsilon_{X\mathrm{R}}\langle d^\dagger_{\mathbf{k}_X-\sigma} c_{\mathbf{q}_\mathrm{R}-\sigma}\rangle) \\ &= \frac{2\mathrm{i}}{N}\sum_{X=\mathrm{I,P}}\sum_{\mathbf{q}_\mathrm{R}\mathbf{k}_X} \epsilon_{\mathbf{k}_\mathrm{R}}\epsilon_{\mathrm{R}X}\,\mathrm{Im}(\langle c^\dagger_{\mathbf{q}_\mathrm{R}-\sigma} d_{\mathbf{k}_X-\sigma}\rangle) \\ &= -\frac{2\mathrm{i}}{N}\sum_{X=\mathrm{I,P}}\sum_{\mathbf{q}_\mathrm{R}\mathbf{k}_X} \epsilon_{\mathbf{k}_\mathrm{R}}\epsilon_{\mathrm{R}X}\,\mathrm{Re}(G^<_{\mathbf{k}_X\mathbf{q}_\mathrm{R}-\sigma}), \end{aligned} \tag{32}$$

where the 'mixed' Green function $G^<_{\mathbf{k}_X\mathbf{q}_\mathrm{R}-\sigma}(t,t') = \mathrm{i}\langle c^\dagger_{\mathbf{q}_\mathrm{R}-\sigma}(t') d_{\mathbf{k}_X-\sigma}(t)\rangle$ was introduced. On the other hand one can show that

$$\begin{aligned} \langle \dot{N}^\sigma_\mathrm{R}\rangle &= \mathrm{i}\langle[H, N^\sigma_\mathrm{R}]_-\rangle \\ &= \mathrm{i}\sum_{\mathbf{q}_\mathrm{R}}\langle[H, \hat{n}_{\mathbf{q}_\mathrm{R}}]_-\rangle \\ &= -2\sum_{X=\mathrm{I,P}}\sum_{\mathbf{q}_\mathrm{R}\mathbf{k}_X} \epsilon_{\mathrm{R}X}\,\mathrm{Re}(G^<_{\mathbf{k}_X\mathbf{q}_\mathrm{R}-\sigma}). \end{aligned} \tag{33}$$

Therefore $B_{1,-\sigma}(\mathbf{k}_\mathrm{R})$ will be proportional to the time-dependent change of total particle number in the right ferromagnet. Since the theory is not explicitly time dependent, this term will always be zero. Thus $B_{1,-\sigma}(\mathbf{k}_\mathrm{R})$ will vanish and can be neglected.

Compared to that of the first band correction, the calculation of $B_{W,-\sigma}(\mathbf{k}_\mathrm{R})$ is quite a bit harder, since it will depend on the wavevector. However, in other works it was shown that this dependence can be neglected without changing the magnetic behaviour of the system very considerably [17]. Thus we will only use the average over all wavevectors:

$$\begin{aligned} B_{W,-\sigma} &\equiv \frac{1}{N}\sum_{\mathbf{k}_\mathrm{R}} B_{W,-\sigma}(\mathbf{k}_\mathrm{R}) \\ &= T_{0,\mathrm{R}}\{n_{\mathrm{R},-\sigma}(1 - n_{\mathrm{R},-\sigma}) - 2\langle \hat{n}_{i_\mathrm{R}-\sigma}\hat{n}_{i_\mathrm{R}\sigma}\rangle\}. \end{aligned} \tag{34}$$

For $i_\mathrm{R} = j_\mathrm{R}$ there is a close resemblance between $B_{W,-\sigma}$ and $B_{S,-\sigma}$. They can be combined to a single-band correction:

$$\begin{aligned} B_{SW,-\sigma} &\equiv B_{S,-\sigma} + B_{W,-\sigma} = -T_{0,\mathrm{R}} n^2_{\mathrm{R},-\sigma} \\ &\quad + \frac{1}{N}\sum_{i_\mathrm{R} j_\mathrm{R}}(T_{i_\mathrm{R} j_\mathrm{R}} - T_{0,\mathrm{R}})\langle c^\dagger_{i_\mathrm{R}-\sigma} c_{j_\mathrm{R}-\sigma}(2\hat{n}_{i_\mathrm{R}\sigma} - 1)\rangle. \end{aligned} \tag{35}$$

The higher correlation function which is part of this band correction can be reduced to a single-particle Green function. In order to show this one first has to multiply

$$\begin{aligned} [H, c^\dagger_{i_\mathrm{R}-\sigma}]_- &= \sum_{l_\mathrm{R}} T_{l_\mathrm{R} i_\mathrm{R}} c^\dagger_{l_\mathrm{R}-\sigma} + U_\mathrm{R}\hat{n}_{i_\mathrm{R}\sigma} c^\dagger_{i_\mathrm{R}-\sigma} \\ &\quad + \sum_{X=\mathrm{I,P}}\sum_{i_X} T_{i_X i_\mathrm{R}} d^\dagger_{i_X-\sigma} \end{aligned} \tag{36}$$

with $c_{j_\mathrm{R}-\sigma}$ from the right and then to form the average to get

$$\begin{aligned} \langle[H, c^\dagger_{i_\mathrm{R}-\sigma}]_- c_{j_\mathrm{R}-\sigma}\rangle &= \sum_{l_\mathrm{R}} T_{l_\mathrm{R} i_\mathrm{R}}\langle c^\dagger_{l_\mathrm{R}-\sigma} c_{j_\mathrm{R}-\sigma}\rangle \\ &\quad + U_\mathrm{R}\langle \hat{n}_{i_\mathrm{R}\sigma} c^\dagger_{i_\mathrm{R}-\sigma} c_{j_\mathrm{R}-\sigma}\rangle + \sum_{X=\mathrm{I,P}}\sum_{i_X} T_{i_X i_\mathrm{R}}\langle d^\dagger_{i_X-\sigma} c_{j_\mathrm{R}-\sigma}\rangle. \end{aligned} \tag{37}$$

On the right-hand side one notices the correlation function of interest, apart from a trivial commutation. With the help of the Heisenberg equation of motion the left-hand side can also be reduced to a one-particle Green function:

$$\begin{aligned} \langle[H, c^\dagger_{i_\mathrm{R}-\sigma}]_-(t) c_{j_\mathrm{R}-\sigma}(t')\rangle &= -\mathrm{i}\frac{\partial}{\partial t}\langle c^\dagger_{i_\mathrm{R}-\sigma}(t) c_{j_\mathrm{R}-\sigma}(t')\rangle \\ &= -\frac{\partial}{\partial t} G^<_{j_\mathrm{R} i_\mathrm{R}-\sigma}(t', t) \\ &= -\frac{1}{2\pi}\frac{\partial}{\partial t}\int_{-\infty}^{\infty} \mathrm{d}E\, G^<_{j_\mathrm{R} i_\mathrm{R}-\sigma}(E)\mathrm{e}^{-\mathrm{i}E(t'-t)} \\ &= -\frac{\mathrm{i}}{2\pi}\int_{-\infty}^{\infty} \mathrm{d}E\, E G^<_{j_\mathrm{R} i_\mathrm{R}-\sigma}(E)\mathrm{e}^{-\mathrm{i}E(t'-t)}. \end{aligned} \tag{38}$$

The two remaining correlation functions can be replaced by lesser Green functions, too:

$$\langle c^\dagger_{l_\mathrm{R}-\sigma}(t) c_{j_\mathrm{R}-\sigma}(t')\rangle = -\frac{\mathrm{i}}{2\pi}\int_{-\infty}^{\infty} \mathrm{d}E G^<_{j_\mathrm{R} l_\mathrm{R}-\sigma}(E)\mathrm{e}^{-\mathrm{i}E(t'-t)} \tag{39}$$

$$\langle d^\dagger_{i_X-\sigma}(t) c_{j_\mathrm{R}-\sigma}(t')\rangle = -\frac{\mathrm{i}}{2\pi}\int_{-\infty}^{\infty} \mathrm{d}E G^<_{j_\mathrm{R} i_X-\sigma}(E)\mathrm{e}^{-\mathrm{i}E(t'-t)}. \tag{40}$$

Putting these equations into the expression (37) for $t = t'$ and transforming to wavevectors leads to

$$\langle \hat{n}_{i_R\sigma} c^{\dagger}_{i_R-\sigma} c_{j_R-\sigma}\rangle = \frac{\mathrm{i}}{2\pi N U_R} \sum_{\mathbf{k}_R} \mathrm{e}^{\mathrm{i}\mathbf{k}_R\cdot(\mathbf{R}_{j_R}-\mathbf{R}_{i_R})} \times \int_{-\infty}^{\infty} \mathrm{d}E \Bigg[(-E+\epsilon_{\mathbf{k}_R}) G^{<}_{\mathbf{k}_R-\sigma}(E) + \sum_{X=\mathrm{I,P}} \sum_{\mathbf{k}_X} G^{<}_{\mathbf{k}_R\mathbf{k}_X-\sigma}(E)\epsilon_{X\mathrm{R}} \Bigg]. \tag{41}$$

The 'mixed' Green function $G_{\mathbf{k}_R\mathbf{k}_X\sigma}$ is closely related to the Green function of the right ferromagnet through the relation

$$\sum_{X=\mathrm{I,P}} \sum_{\mathbf{k}_X} G_{\mathbf{k}_R\mathbf{k}_X\sigma}\epsilon_{X\mathrm{R}} = G_{\mathbf{k}_R\sigma}\Delta_{\mathbf{k}_R\sigma}. \tag{42}$$

Applying the analytic continuation rules given by Langreth [15, 18] to this equation to get its lesser component yields

$$\sum_{X=\mathrm{I,P}} \sum_{\mathbf{k}_X} G^{<}_{\mathbf{k}_R\mathbf{k}_X\sigma}\epsilon_{\mathbf{k}_X\mathbf{k}_R} = G^{\mathrm{r}}_{\mathbf{k}_R\sigma}\Delta^{<}_{\mathbf{k}_R\sigma} + G^{<}_{\mathbf{k}_R\sigma}\Delta^{a}_{\mathbf{k}_R\sigma}. \tag{43}$$

Thus the integral core can be written as

$$\begin{aligned}&[(-E+\epsilon_{\mathbf{k}_R})G^{<}_{\mathbf{k}_R-\sigma} + \sum_{X=\mathrm{I,P}}\sum_{\mathbf{k}_X} G^{<}_{\mathbf{k}_R\mathbf{k}_X-\sigma}\epsilon_{X\mathrm{R}}] \\ &= (-E+\epsilon_{\mathbf{k}_R}+\Delta^{\mathrm{r}}_{\mathbf{k}_R-\sigma})G^{<}_{\mathbf{k}_R-\sigma} \\ &\quad + G^{\mathrm{r}}_{\mathbf{k}_R-\sigma}\Delta^{<}_{\mathbf{k}_R-\sigma}G^{a}_{\mathbf{k}_R-\sigma}(G^{a}_{\mathbf{k}_R-\sigma})^{-1} \\ &= -\Sigma^{a}_{\mathbf{k}_R-\sigma}G^{<}_{\mathbf{k}_R-\sigma}\end{aligned} \tag{44}$$

which leads to the following expression for the correlation function:

$$\langle \hat{n}_{i_R\sigma} c^{\dagger}_{i_R-\sigma} c_{j_R-\sigma}\rangle = -\frac{\mathrm{i}}{2\pi N U_R} \sum_{\mathbf{k}_R} \mathrm{e}^{\mathrm{i}\mathbf{k}_R\cdot(\mathbf{R}_{j_R}-\mathbf{R}_{i_R})} \times \int_{-\infty}^{\infty} \mathrm{d}E\, \Sigma^{a}_{\mathbf{k}_R-\sigma}(E) G^{<}_{\mathbf{k}_R-\sigma}(E). \tag{45}$$

Therefore the band correction $B_{SW,-\sigma}$ reads

$$B_{SW,-\sigma} = -T_{0,\mathrm{R}} n^2_{\mathrm{R},-\sigma} - \frac{\mathrm{i}}{2\pi N}\sum_{\mathbf{k}_R}(\epsilon_{\mathbf{k}_R}-T_{0,\mathrm{R}}) \times \int_{-\infty}^{\infty} \mathrm{d}E \Bigg[\left(\frac{2}{U_R}\Sigma^{a}_{\mathbf{k}_R-\sigma}(E) - 1\right) G^{<}_{\mathbf{k}_R-\sigma}(E) \Bigg]. \tag{46}$$

The last remaining band correction is $B_{T,-\sigma}$. Its structure is very similar to that of $B_{SW,-\sigma}$. Thus the calculation of the higher correlation function runs along the same lines as were shown above. For the sake of brevity we will not go into the details of this calculation. The result is

$$B_{T,-\sigma} = -\frac{\mathrm{i}}{2\pi N}\sum_{\mathbf{k}_R}\int_{-\infty}^{\infty}\mathrm{d}E \Bigg[(E-\epsilon_{\mathbf{k}_R}-\Sigma^{a}_{\mathbf{k}_R-\sigma}(E)) \times \left(\frac{2}{U_R}\Sigma^{\mathrm{r}}_{\mathbf{k}_R-\sigma}(E)-1\right) G^{<}_{\mathbf{k}_R-\sigma}(E) + \frac{2}{U_R}\Delta^{<}_{\mathbf{k}_R-\sigma}(E) \Bigg]. \tag{47}$$

All non-vanishing band corrections which are part of the third moment can be merged into a single one which we call $B_{\mathrm{R},-\sigma}$:

$$\begin{aligned} n_{\mathrm{R},-\sigma}(1-n_{\mathrm{R},-\sigma})B_{\mathrm{R},-\sigma} &\equiv T_{0,\mathrm{R}} n^2_{\mathrm{R},-\sigma} + B_{SW,-\sigma} + B_{T,-\sigma} \\ &= -\frac{\mathrm{i}}{2\pi N}\sum_{\mathbf{k}_R}\int_{-\infty}^{\infty}\mathrm{d}E \Bigg[\left(\frac{2}{U_R}\Sigma^{\mathrm{r}}_{\mathbf{k}_R-\sigma}(E)-1\right) \\ &\quad \times (E-T_{0,\mathrm{R}}-\Sigma^{\mathrm{r}}_{\mathbf{k}_R-\sigma}(E))G^{<}_{\mathbf{k}_R-\sigma}(E) + \frac{2}{U_R}\Delta^{<}_{\mathbf{k}_R-\sigma}(E) \Bigg]. \end{aligned} \tag{48}$$

Thus the first four moments of the right ferromagnet are known. For the determination of the self-energy one additionally needs the first three moments of the transport self-energy. It can be split into two parts which describe the coupling to the insulator and the paramagnet, respectively:

$$\begin{aligned}\Delta^{\mathrm{r}}_{\mathbf{k}_R\sigma}(E) &= \sum_{\mathbf{k}_I}\epsilon^2_{\mathrm{RI}}G^{(\mathrm{L}),\mathrm{r}}_{\mathbf{k}_I\sigma}(E) + \sum_{\mathbf{k}_P}\epsilon^2_{\mathrm{RP}}g^{\mathrm{r}}_{\mathbf{k}_P\sigma}(E) \\ &= \sum_{m=0}^{\infty}\frac{\sum_{X=\mathrm{I,P}}\sum_{\mathbf{k}_X}\epsilon^2_{\mathrm{R}X}M^{(m)}_{\mathbf{k}_X\sigma}}{E^{m+1}} \\ &\stackrel{!}{=} \sum_{m=0}^{\infty}\frac{D^{(m)}_{\mathbf{k}_R\sigma}}{E^m}.\end{aligned} \tag{49}$$

The first two moments of both the insulator and the paramagnet are almost trivial. For $X = \mathrm{I, P}$ one finds

$$M^{(0)}_{\mathbf{k}_X\sigma} = 1, \qquad M^{(1)}_{\mathbf{k}_X\sigma} = \epsilon_{\mathbf{k}_X}. \tag{50}$$

By comparison with these moments the first three $D^{(m)}_{\mathbf{k}_R\sigma}$ can be easily determined:

$$D^{(0)}_{\mathbf{k}_R\sigma} = 0 \tag{51}$$

$$D^{(1)}_{\mathbf{k}_R\sigma} = \sum_{X=\mathrm{I,P}}\epsilon^2_{\mathrm{R}X} \tag{52}$$

$$D^{(2)}_{\mathbf{k}_R\sigma} = \sum_{X=\mathrm{I,P}}\epsilon^2_{\mathrm{R}X}T_{0,X}. \tag{53}$$

This is all the information that one needs to calculate the coefficients of the interaction self-energy. Putting the moments into equations (19)–(21) yields

$$C^{(0)}_{\mathbf{k}_R\sigma} = U_R n_{\mathrm{R},-\sigma} \tag{54}$$

$$C^{(1)}_{\mathbf{k}_R\sigma} = U^2_R n_{\mathrm{R},-\sigma}(1-n_{\mathrm{R},-\sigma}) \tag{55}$$

$$C^{(2)}_{\mathbf{k}_R\sigma} = U^2_R n_{\mathrm{R},-\sigma}(1-n_{\mathrm{R},-\sigma})(B_{\mathrm{R},-\sigma}+T_{0,\mathrm{R}}) + U^3_R n_{\mathrm{R},-\sigma}(1-n_{\mathrm{R},-\sigma})^2. \tag{56}$$

For high energies it is permissible to restrict the expansion (18) to the lowest orders of $1/E$. Therefore the following approximation should be valid in this limit:

$$\begin{aligned}\Sigma^{\mathrm{r}}_{\mathbf{k}_R\sigma}(E) &= C^{(0)}_{\mathbf{k}_R\sigma} + \frac{C^{(1)}_{\mathbf{k}_R\sigma}}{E} + \frac{C^{(2)}_{\mathbf{k}_R\sigma}}{E^2} + \cdots \\ &= C^{(0)}_{\mathbf{k}_R\sigma} + \frac{C^{(1)}_{\mathbf{k}_R\sigma}}{E}\left(1 + \frac{C^{(2)}_{\mathbf{k}_R\sigma}}{C^{(1)}_{\mathbf{k}_R\sigma}E} + \cdots\right) \\ &\approx C^{(0)}_{\mathbf{k}_R\sigma} + \frac{C^{(1)}_{\mathbf{k}_R\sigma}}{E - \frac{C^{(2)}_{\mathbf{k}_R\sigma}}{C^{(1)}_{\mathbf{k}_R\sigma}}} \\ &= U_R n_{\mathrm{R},-\sigma}\frac{E - B_{\mathrm{R},-\sigma} - T_{0,\mathrm{R}}}{E - B_{\mathrm{R},-\sigma} - T_{0,\mathrm{R}} - U_R(1-n_{\mathrm{R},-\sigma})}.\end{aligned} \tag{57}$$

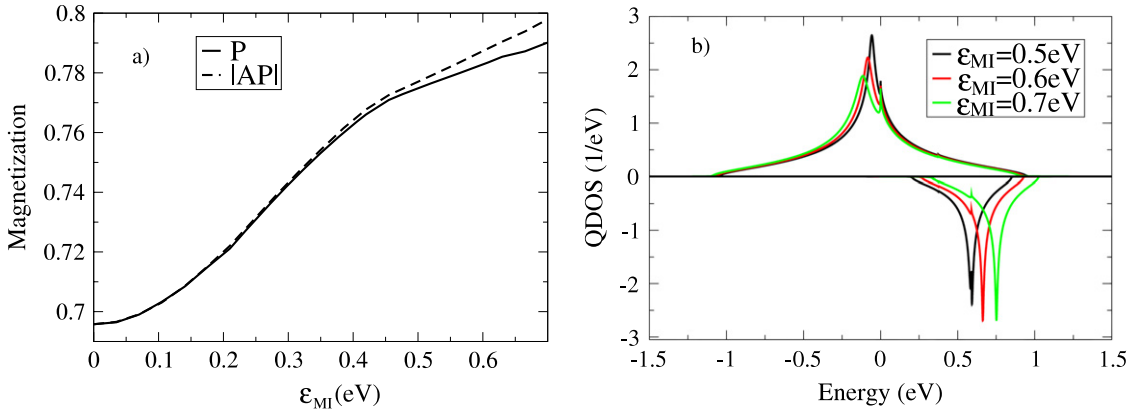

Figure 2. (a) Magnetization of the right ferromagnet as a function of the strength of hybridization ϵ_{MI} between the insulator and the ferromagnets without applied voltage. For comparison reasons the absolute value of the antiparallel magnetization is shown. (b) The QDOS of the right ferromagnet for different hybridization strengths and parallel alignment. Only the lower Hubbard bands are shown. Parameters from table 1 were used.

This is the main result for the NSDA self-energy. It formally coincides with the equilibrium spectral density approximation (SDA) [19], but they are by no means equal, because of the band correction $B_{\mathrm{R},-\sigma}$. In equilibrium it can be calculated using

$$n_{\mathrm{R},-\sigma}(1-n_{\mathrm{R},-\sigma})B^{\mathrm{SDA}}_{\mathrm{R},-\sigma} = \frac{1}{N}\sum_{\mathbf{k}_\mathrm{R}}(\epsilon_{\mathbf{k}_\mathrm{R}} - T_{0,\mathrm{R}}) \times \int_{-\infty}^{\infty} \mathrm{d}E f_\mathrm{R}(E)\left(\frac{2}{U_\mathrm{R}}(E-\epsilon_{\mathbf{k}_\mathrm{R}})-1\right) S_{\mathbf{k}_\mathrm{R}-\sigma}(E), \quad (58)$$

which is obviously not the same as (48). However, one can show that the NSDA band correction is reduced to (58) in the equilibrium limit $\epsilon_{MI}, \epsilon_{\mathrm{RP}} \to 0$, i.e. the SDA is a limiting case of the NSDA.

4. Numerical results

For the numerical evaluation of the theory we used the mean field approximation for the left ferromagnet, $\Sigma^{\mathrm{r}}_{\mathbf{k}_\mathrm{L}\sigma}(E) = U_\mathrm{L} n_{\mathrm{L},-\sigma}$. On choosing U_L large it will become a half-metal, i.e. only electrons of one spin direction are present near the Fermi energy. The spin axis of the left ferromagnet is chosen as fixed, so its majority electrons will always be spin up. Thus its magnetization is positive. The right ferromagnet is aligned parallel (antiparallel) to the left one if its magnetization is positive (negative). We already showed that the proposed theory is indeed able to model current-induced switching of magnetization in another paper [13]. The magnetization shows a hysteresis-like behaviour in the dependence on the applied voltage. This can be explained in terms of the quasiparticle density of states (QDOS) of the two ferromagnets. A hybridization between two bands will lead to a repulsion between them. How strong this repulsion will be depends on three factors: the hybridization strength, the energetic distance of the bands and their spectral weight. The repulsion only acts between bands with the same spin. With these observations it is possible to completely explain the magnetization behaviour.

In this paper we want to study the parameter dependences of the magnetization and their influence on the switching behaviour. The variation of the critical current which changes the sign of the magnetization is of special interest. It can be plotted in the form of a phase diagram where regions with parallel and antiparallel alignment are shown. At least in principle, one has to plot two phase diagrams for each parameter, one starting with parallel the other with antiparallel alignment. On the other hand, one voltage semiaxis would always be trivial, since e.g. for parallel orientation positive voltages are never able to switch the magnetization. The phase diagram would consist of one phase only. The same holds for antiparallel alignment and negative voltages. Therefore one can combine the two phase diagrams into a single one by leaving out the uninteresting single-phase regions. In the resulting phase diagram positive (negative) voltages mean that the calculation was started with antiparallel (parallel) orientation.

4.1. The hybridization strength

The magnetization of the right ferromagnet without any applied voltage is shown in figure 2. For vanishing hybridization strength, $\epsilon_{MI} = 0$ eV, it is identical for the two alignments. Since in this case the ferromagnet is only coupled to the paramagnet, this is to be expected, because there is no preferred orientation for the spin. Therefore the distinction between parallel and antiparallel becomes meaningless. The only difference between the magnetizations is their sign. With increasing hybridization strength the magnetization increases for both alignments. For small ϵ_{MI} the curves are almost identical. Above $\epsilon_{MI} \approx 0.3$ eV a small splitting becomes visible which gets enhanced above $\epsilon_{MI} \approx 0.45$ eV. For higher hybridization strengths both magnetizations grow approximately linearly and the slope of the antiparallel curve is slightly higher. The reason for this increase is the repulsion between left and right spin up bands. It will be stronger for higher hybridization. For antiparallel orientation the right spin up band will be above the left one,

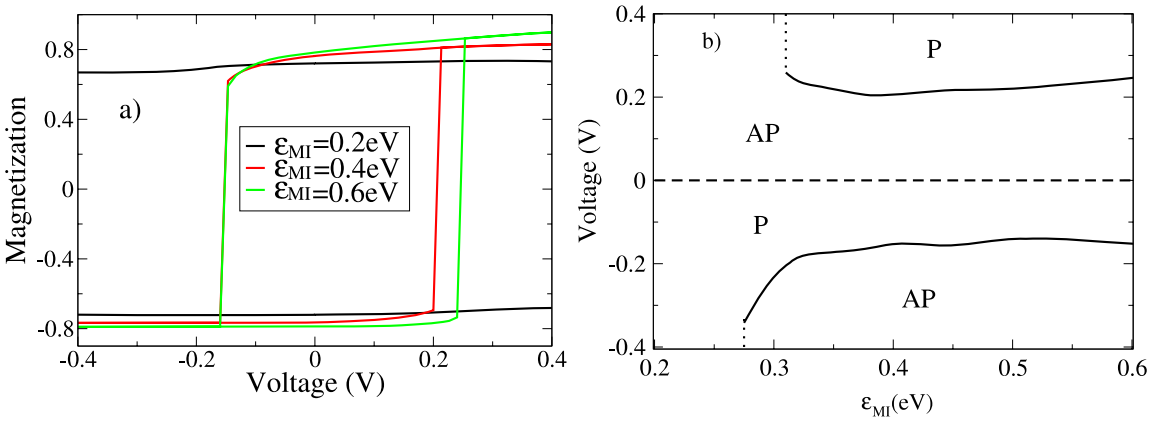

Figure 3. (a) Voltage-dependent magnetization curves of the right ferromagnet for different hybridization strengths ϵ_{MI}. (b) Dependence of the critical voltage on the hybridization strength. Positive voltages start from parallel, negative voltages from antiparallel alignment. The cases of positive (negative) voltages starting with parallel (antiparallel) alignment are not shown because they are trivial since the phases are always stable, as can be seen in the left figure. Parameters from table 1 were used.

so growing ϵ_{MI} will move it to higher energies. Since spin up is the minority spin direction in the right ferromagnet in this situation, this results in an increase of the magnetization. For parallel orientation both spin up bands lie at the same energy. Therefore there is no big movement of the whole band, but only a dislocation of spectral weight away from the common centre of gravity which can be seen in figure 2. Thus the magnetization will increase in this case, too, but not so strongly as for antiparallel alignment. However, the relative difference between the two orientations is not very large.

If the hybridization strength is too low, the $V = 0$ phases remain stable. This can be seen for the $\epsilon = 0.2$ eV curve in the left picture of figure 3 and also, in a more systematic way, in the phase diagram on the right. There is only a small change of magnetization: for negative voltages it is slightly reduced, while for positive voltages it is increased. But this change is not strong enough to destabilize the system. Only if the hybridization exceeds a certain value will it be possible to change the direction of magnetization by applying a voltage. Since the current is proportional to the hybridization strength that means that there is a critical current below which it will not be possible to switch the magnetization. This is in agreement with experimental observations [20]. The critical hybridization strength is slightly lower for parallel alignment than for antiparallel orientation ($\epsilon_{MI} = 0.27$ eV compared to $\epsilon_{MI} = 0.31$ eV). This disagreement is caused by the already mentioned fact that in the parallel case the current is determined by the majority bands while in the antiparallel case it will be carried by the minority band. This leads to a lower current, and thus a higher hybridization strength is needed to reach the critical current density. After switching becomes possible above the critical threshold, a further increase of ϵ_{MI} will lower the critical voltage, so a reorientation of the magnetization will be easier. For higher hybridizations this behaviour is reversed again, i.e. the switching point moves to higher voltages. This is caused by an increase of the magnetization itself as can be seen in figure 2. One should note the asymmetric behaviour of the magnetization: the transition from parallel to antiparallel is only possible for negative voltages, while the inverse transition happens for positive voltages only. This is one of the hallmarks of current-induced switching of magnetization [21].

Table 1. Standard parameters. In all subsequent calculations these values were used, unless stated otherwise.

Occupation number	$n = 0.7$
Coulomb interaction strength (eV)	$U_{\mathrm{L}} = 20$ $U_{\mathrm{R}} = 4$
Hybridization strength (eV)	$\epsilon_{MI} = 0.5$ $\epsilon_{\mathrm{RP}} = 0.05$
Centre of gravity (eV)	$T_{0,I} = 5$ $T_{0,\mathrm{R}} = T_{0,\mathrm{L}} = 0$
Bandwidth (eV)	$W_{\mathrm{L}} = 3$ $W_{\mathrm{I}} = 1$ $W_{\mathrm{R}} = 2$ $W_{\mathrm{P}} = 5$
Temperature (K)	$T = 0$

4.2. The Coulomb interaction strength

The dependence of the magnetization of the right ferromagnet on the Coulomb interaction strength U_{R} is shown in figure 4. A critical $U_{\mathrm{R,c}} \approx 1$ eV will be necessary to get a finite magnetization for both alignments. Above this critical interaction strength the magnetization strongly increases and will go into saturation for higher U_{R}. Compared to the (equilibrium) SDA magnetization, which is shown as a dotted line, the NSDA has a smaller critical interaction strength and the transition to saturation is much faster. Also the saturation value is higher. The last point is a consequence of the fact that the occupation number of the right ferromagnet is not fixed in nonequilibrium, contrary to the equilibrium case. The value of $n_{\mathrm{R}} = n_{\mathrm{R},\uparrow} + n_{\mathrm{R},\downarrow}$ is a result of the position of the chemical potentials in the two leads. For $n = 0.7$ in the leads we find $n_{\mathrm{R}} = 0.77$ for the right ferromagnet which is exactly the saturation value of the magnetization. The relative orientation of the magnetization plays no important

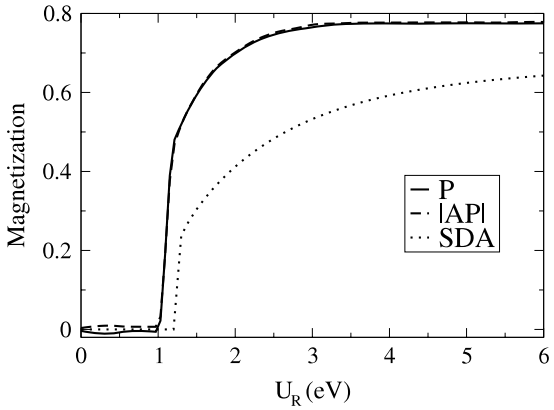

Figure 4. Magnetization of the right ferromagnet for both alignments as a function of Coulomb interaction strength U_R without applied voltage. For comparison reasons the absolute value of the antiparallel magnetization is shown. The dotted line is the equilibrium SDA magnetization. Parameters from table 1 were used.

role since the P and AP curves are virtually identical. Both orientations behave in a similar way to the SDA, with the above mentioned differences. The higher magnetic stability of the nonequilibrium system results from the coupling to the fully polarized left ferromagnet. This will obviously increase the probability for creating a spin asymmetry in the right ferromagnet.

The voltage-dependent magnetization curves and the corresponding phase diagram are shown in figure 5. Since the right ferromagnet does not have a finite magnetization below $U_R = 1$ eV, there cannot be switching below this value either. However, due to the current the magnetization will be non-zero if a voltage is applied. For positive voltages spin up electrons will flow from the left to the right ferromagnet, resulting in a positive magnetization, i.e. parallel alignment. For negative voltages the situation is reversed, which leads to antiparallel orientation as can be seen in the phase diagram.

Above $U_R = 1$ eV there will be a finite magnetization for both alignments, even without an applied voltage. For all higher Coulomb interaction strengths the system will show a transition from antiparallel to parallel for positive voltages and from parallel to antiparallel for negative voltages, respectively. Both from the voltage-dependent magnetization curves and from the phase diagram one can conclude that the critical voltage needed for switching the magnetization increases with increasing U_R. Since the right magnetization also grows with increasing U_R this is a direct consequence of the higher magnetic stability of the system. Therefore higher voltages (currents) are needed for a reorientation.

5. Conclusion

We developed a microscopic model of a magnetic tunnel junction for the description of current-induced switching of magnetization. The ferromagnets were described using the single-band Hubbard model and the coupling between the regions was simulated by a hybridization between neighbouring bands. Since the Hubbard model is not exactly solvable we further developed the so-called NSDA which allows a self-consistent calculation of the magnetization taking into account interactions beyond the mean field level. For the numerical evaluation the left ferromagnet was treated in the mean field approximation and the right one in the NSDA. It was shown that the repulsion between the bands due to the hybridization is responsible for getting the switching behaviour. The dependence of the critical voltage at which the magnetization switches its sign on the model parameters can be studied in a systematic way. We presented results for a variation of the hybridization strength ϵ_{MI} and the Coulomb interaction strength U_R of the switching magnet. The results indicate that a certain critical ϵ_{MI} is necessary to get switching. This is in qualitative agreement with experiment, because the tunnelling current is also proportional to ϵ_{MI}. With increasing U_R the magnetic stability of the ferromagnet is enhanced. Thus switching will be more difficult. This is also an expected result. Therefore we conclude that the model is indeed able to qualitatively describe the phenomenon of current-induced switching of magnetization.

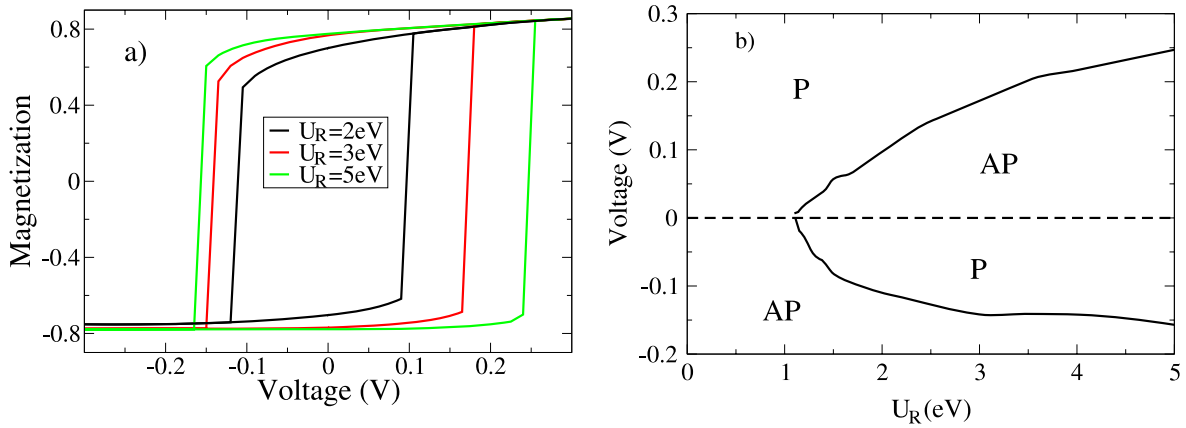

Figure 5. Left: voltage-dependent magnetization curves of the right ferromagnet for different Coulomb interaction strengths U_R. Right: dependence of the critical voltage on U_R. Positive voltages start from parallel, negative voltages from antiparallel alignment. Parameters from table 1 were used.

References

[1] Slonczewski J 1996 *J. Magn. Magn. Mater.* **159** L1
[2] Berger L 1996 *Phys. Rev.* B **54** 9353
[3] Tsoi M, Jansen A G M, Bass J, Chiang W-C, Seck M, Tsoi V and Wyder P 1998 *Phys. Rev. Lett.* **80** 4281
[4] Myers E B, Ralph D C, Katine J A, Louie R N and Buhrman R A 1999 *Science* **285** 867
[5] Grollier J, Cros V, Hamzic A, George J M, Jaffres H, Fert A, Faini G, Ben Youssef J and Legall H 2001 *Appl. Phys. Lett.* **78** 3663
[6] Duine R A, Nunez A S, Sinova J and MacDonald A H 2007 *Phys. Rev.* B **75** 214420
[7] Edwards D M, Federici F, Mathon J and Umerski A 2005 *Phys. Rev.* B **71** 054407
[8] Sun J Z 2006 *IBM J. Res. Dev.* **50** 81
[9] Weinberger P, Vernes A, Györffy B L and Szunyogh L 2004 *Phys. Rev.* B **70** 094401
[10] Zhang S, Levy P M and Fert A 2002 *Phys. Rev. Lett.* **88** 236601
[11] Hickey M and Moodera J 2009 *Phys. Rev. Lett.* **102** 137601
[12] Hankiewicz E M, Vignale G and Tserkovnyak Y 2007 *Phys. Rev.* B **75** 174434
[13] Sandschneider N and Nolting W 2009 *Phys. Rev.* B **79** 184423
[14] Keldysh L V 1964 *Zh. Eksp. Teor. Fiz.* **47** 1515
Keldysh L V 1965 *Sov. Phys.—JETP* **20** 1018 (Engl. Transl.)
[15] Haug H and Jauho A-P 2007 *Quantum Kinetics in Transport and Optics of Semiconductors* (Berlin: Springer)
[16] Ng T K 1993 *Phys. Rev. Lett.* **70** 3635
[17] Herrmann T and Nolting W 1997 *J. Magn. Magn. Mater.* **170** 253
[18] Langreth D C 1976 *Linear and Nonlinear Electron Transport in Solids* (*NATO Advanced Study Institute Series B*) (New York: Plenum)
[19] Nolting W and Borgiel W 1989 *Phys. Rev.* B **39** 6962
[20] Huai Y, Albert F, Nguyen P, Pakala M and Valet T 2004 *Appl. Phys. Lett.* **84** 3118
[21] Heide C, Zilberman P E and Elliott R J 2001 *Phys. Rev.* B **63** 064424